Proc. Natl. Acad. Sci. USA
Vol. 87, pp. 5243–5247, July 1990
Biochemistry

Crystal structure of fructose-1,6-bisphosphatase complexed with fructose 6-phosphate, AMP, and magnesium

(x-ray crystallography/allosteric enzyme/active site/quaternary structure changes)

HENGMING KE, YIPING ZHANG, AND WILLIAM N. LIPSCOMB

Gibbs Chemical Laboratory, Harvard University, 12 Oxford Street, Cambridge, MA 02138

Contributed by William N. Lipscomb, May 3, 1990

ABSTRACT **The crystal structure of fructose-1,6-bisphosphatase (EC 3.1.3.11) complexed with fructose 6-phosphate, AMP, and Mg^{2+} has been solved by the molecular replacement method and refined at 2.5-Å resolution to a *R* factor of 0.215, with root-mean-square deviations of 0.013 Å and 3.5° for bond lengths and bond angles, respectively. No solvent molecules have been included in the refinement. This structure shows large quaternary and tertiary conformational changes from the structures of the unligated enzyme or its fructose 2,6-bisphosphate complex, but the secondary structures remain essentially the same. Dimer C3–C4 of the enzyme–fructose 6-phosphate–AMP–Mg^{2+} complex twists about 19° relative to the same dimer of the enzyme–fructose 2,6-bisphosphate complex if their C1–C2 dimers are superimposed on one another. Nevertheless, many interfacial interactions between dimers of C1–C2 and C3–C4 are conserved after quaternary structure changes occur. Residues of the AMP domain (residues 6–200) show large migrations of Cα atoms relative to barely significant positional changes of the FBP domain (residues 201–335).**

Fructose-1,6-bisphosphatase (Fru-1,6-Pase; D-fructose-1,6-bisphosphate 1-phosphohydrolase, EC 3.1.3.11), a key regulatory enzyme in gluconeogenesis, catalyzes the hydrolysis of fructose 1,6-bisphosphate to fructose 6-phosphate (F6*P*) and inorganic phosphate. Fru-1,6-Pase isolated from various sources consisted of four identical polypeptide chains that aggregate into a relatively flat tetramer (Fig. 1). Seven complete amino acid sequences have been reported for Fru-1,6-Pases from various sources (1–6). Recently, three-dimensional structures of the unligated Fru-1,6-Pase and of its complex with fructose 2,6-bisphosphate (Fru-2,6-P_2) in the space group $P3_221$ were described in detail (7, 8*).

The catalytic and regulatory properties of the enzyme isolated from gluconeogenic tissues as well as other sources have been extensively studied (9, 10). Omitting those forms that also have a phosphorylation site, the enzyme activity is regulated *in vivo* by Fru-2,6-P_2 and AMP (9, 10). Kinetic experiments controversially have suggested that Fru-2,6-P_2 binds to the active site (11), to an allosteric site (12), or to both (13). On basis of the structures, we proposed that Fru-2,6-P_2 binds to the active site (7, 8). AMP is an allosteric inhibitor (14), and its inhibition is synergistic with Fru-2,6-P_2 (15, 16).

We have grown cocrystals of the enzyme complexed with F6*P*, AMP, and Mg^{2+} in the space group $P2_12_12$. This structure† has been solved by the molecular replacement method and shows large quaternary and tertiary conformational changes from the unligated structure or the structure of the enzyme–Fru-2,6-P_2 complex. Here, we describe the F6*P* and AMP binding sites and large structural differences between the enzyme–F6*P*–AMP–Mg^{2+} complex and the enzyme–Fru-2,6-P_2 complex.

The publication costs of this article were defrayed in part by page charge payment. This article must therefore be hereby marked "*advertisement*" in accordance with 18 U.S.C. §1734 solely to indicate this fact.

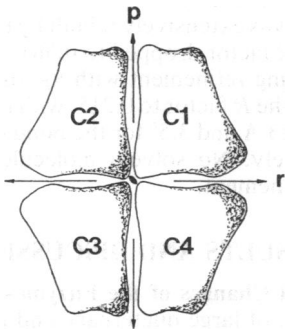

FIG. 1. Schematic diagram of Fru-1,6-Pase looking down a molecular twofold axis (labeled ◥ in the center of the diagram or *q* in Fig. 4). The other two molecular twofold axes are labeled *p* (vertical) and *r* (horizontal). The molecule has D_2 symmetry. Subunits C1 and C2 make up the crystallographic asymmetric unit.

METHODS

Fru-1,6-Pase was purified from pig kidney as described (8). It has an optimal activity at neutral pH. The neutral form of Fru-1,6-Pase was cocrystallized with 1 mM AMP, 1 mM F6*P*, and 5 mM $MgCl_2$ by dialyzing a protein solution (10–15 mg/ml) against a buffer containing 20 mM Tris base, 2 mM maleic acid, 0.1 mM EDTA, 5 mM NaN_3, and 9.5% (wt/vol) PEG (molecular weight = 3350) at pH 7.4. A 4- to 7-day dialysis yielded crystals with a typical size of 0.3 × 0.8 × 1.5 mm, which have the space group $P2_12_12$ with unit cell dimensions of a = 61.6, b = 166.6, and c = 80.0 Å. Two monomers exist in the crystallographic asymmetric unit.

The diffraction data were collected on the multiwire x-ray area detector at the Biotechnology Resource, University of Virginia (17). A total of 87,690 measured diffraction maxima was reduced to 27,511 unique reflections with a R_{sym} of 6.1%. These data are nearly complete to 2.5-Å resolution and also include 856 reflections at higher resolution.

The recently refined structure of the enzyme–F6*P* complex (H.K. and W.N.L., unpublished results) in the space group $P3_221$ was used to find the orientation of the enzyme–F6*P*–AMP–Mg^{2+} structure in the space group $P2_12_12$. To do so, a dimer of the F6*P* structure was placed in a large artificial *P*1 cell in order to obtain structure factors; Crowther's cross rotation function (18) was then calculated for several resolution shells with different intensity cutoff values. These calculations for different shells consistently indicated the strongest peak at $\alpha = 45°$, $\beta = 85°$, and $\gamma = -65°$. The *R*-factor search was carried out by use of the translation function (19)

Abbreviations: Fru-1,6-Pase, fructose-1,6-bisphosphatase; Fru-2,6-P_2, fructose 2,6-bisphosphate; F6*P*, fructose 6-phosphate.

*In this paper, the stereoviews of figures 10 and 13, but not the legends, should be interchanged.

†The atomic coordinates have been deposited in the Protein Data Bank, Chemistry Department, Brookhaven National Laboratory, Upton, NY 11973 (reference 1FBP).

for various resolution shells from 5 to 8 Å. The correct solution from the *R*-factor search, which had the lowest *R* factor (0.405) for 606 reflections, was further distinguished from others by examination of lattice contacts by using the program FRODO (20).

Taken as two rigid bodies, one for each monomer, the model from the molecular replacement was refined for 40 steps of energy minimization by using the program XPLOR (21). This refinement decreased the *R* factor from 0.539 to 0.392 for 25,402 reflections between 10.0- and 2.5-Å resolution. This rigid body refinement showed a maximum of 5.4° of rotation, which was different from that of the molecular replacement, and up to 3° of difference between relative rotation of two monomers. After the structure from the rigid body refinement was extensively rebuilt by using the program FRODO (20), the *R* factor dropped to 0.364. Several cycles of simulated annealing refinement with XPLOR and manual rebuilding brought the *R* factor to 0.215, with root-mean-square deviations of 0.013 Å and 3.5° for the bond lengths and bond angles, respectively. No solvent molecules have been included in the refinement.

RESULTS AND DISCUSSION

Conformational Changes of the Enzyme–F6*P*–AMP–Mg^{2+} Complex. In spite of large quaternary and tertiary structure changes, the secondary structures of the enzyme–F6*P*–AMP–Mg^{2+} complex remain essentially the same as those of the enzyme–Fru-2,6-P_2 complex. Similar to the unligated structure (Fig. 2), we also find here that the loop of residues 54–67 and the N-terminal region (residues 1–5) in the structure of the F6*P*–AMP–Mg^{2+} complex show little or no electron density. Thus the loop of residues 54–67 might exist in multiple conformations, might be disordered, or might have been removed partially or completely by proteolytic cleavage. This region is proteolytically sensitive (22). No significant cleavages were detected by microsequencing techniques in a solution prepared by redissolving our crystals. It is therefore most probable that this loop has multiple conformations or more extensive disorder.

In Fig. 3, we show plots of Cα positions of the Fru-2,6-P_2 complex (Fig. 3 *Left*) and the F6*P*–AMP–Mg^{2+} complex (Fig. 3 *Right*), projecting along the molecular twofold axis *p* (vertical in Fig. 1). This view shows the major change in molecular shape. In this projection, dimer C1–C2 extends from the lower right corner to the upper left corner as it crosses dimers C3–C4. If dimer C1–C2 of the F6*P*–AMP–Mg^{2+} complex is superimposed on the same dimer of the Fru-2,6-P_2 complex, dimers C3–C4 differ in orientation about the molecular twofold axis *p* (vertical in Fig. 1) by about 19° relative to one another. Consequently, the molecular twofold axes *r* and *q* rotate about 9.5° (Fig. 4) when the Fru-2,6-P_2 complex transforms to the structure of the F6*P*–AMP–Mg^{2+} complex. Surprisingly, many of the interfacial interactions between dimers C1–C2 and C3–C4 are conserved after this large quaternary structural change takes place. Residues of the AMP domain (residues 6–200) significantly migrate in such a way that these interfacial interactions are maintained. On average, the AMP domain shows a shift of 0.93 Å for Cα atoms, in contrast to a shift of 0.39 Å for the FBP domain (residues 201–335). A detailed comparison of the quaternary and tertiary structures will be discussed elsewhere.

Binding Site for F6*P*. In the ($F_0 - F_c$) map calculated from the rigid body refinement omitting AMP, F6*P*, and Mg^{2+}, there are three pairs of strong peaks for the dimer in the crystallographic asymmetric unit. The site for Mg^{2+} can be recognized from the character of smallest and strongest pieces of electron density among these three pairs. Also, it is easy to distinguish the F6*P* site from the AMP site by the shape of density since AMP has a purine base, which is much bigger than the hydroxyl group of F6*P*.

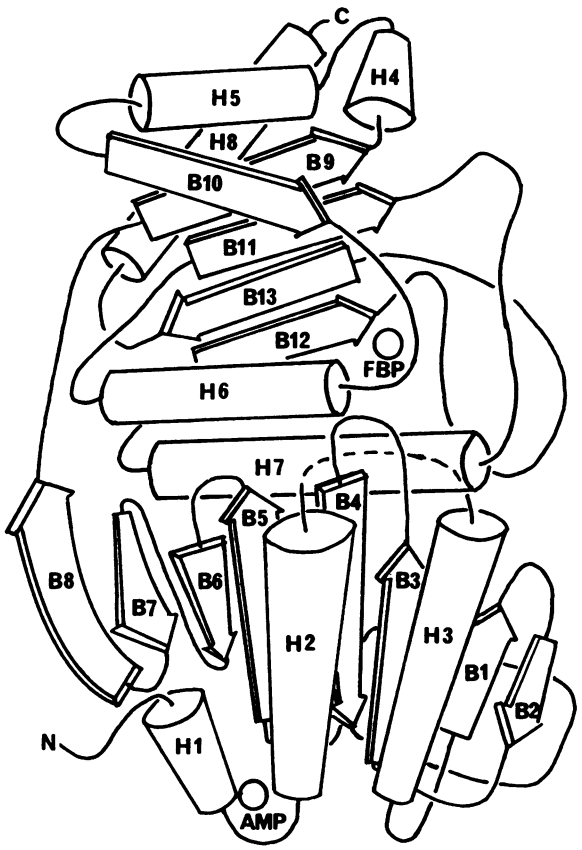

FIG. 2. Secondary structure of a monomer of Fru-1,6-Pase. The letters N and C represent the N and C termini, respectively. The α-helices are shown as cylinders, and the β-strands are shown as arrows. The dashed line between H2 and H3 represents the missing loop of Ala-54 to Gly-67. The circles labeled FBP and AMP indicate the active site and the AMP binding location of the enzyme, respectively.

As shown in Fig. 5, the 6-phosphate group of F6*P* interacts with side chain atoms of Asn-212, Tyr-215, Tyr-244, Tyr-264, and Lys-274 in the same monomer and Arg-243 from the neighboring monomer. Arg-269 is near the phosphate group, although its poor electron density may imply partial disordered conformations. The sugar ring of F6*P* contacts side chain atoms of Lys-274 and backbone atoms of Ser-247 and Met-248. Divalent metal Mg^{2+} is located in the negatively charged pocket, coordinating with side chain atoms of Glu-97, Asp-118, Asp-121, and Glu-280. This Mg^{2+} site has the same binding contacts as does the Mg^{2+} complex in the absence of both AMP and F6*P* (8).

The proposed site or sites to which Fru-2,6-P_2 binds to the enzyme include the active site (11), the allosteric site (12), and both catalytic and allosteric sites (13). Our x-ray diffraction studies indicate that Fru-2,6-P_2 binds at the active site of the enzyme (7, 8). The present study shows that the 6-phosphate and sugar groups of F6*P* binds at the active site in positions that correspond to the 6-phosphate and ribose of Fru-2,6-P_2 in our previous studies.

Binding Site for AMP. Two strong peaks in the crystallographic asymmetric unit of either ($2F_o - F_c$) or ($F_o - F_c$) map suggest four sites per tetramer or one site per monomer for binding of AMP to the neutral form of the enzyme. These peaks are located at the AMP binding location that we previously reported (7). However, our previous study shows only two major sites per tetramer, instead of four sites , for AMP binding. The difference may be related to the quality of the

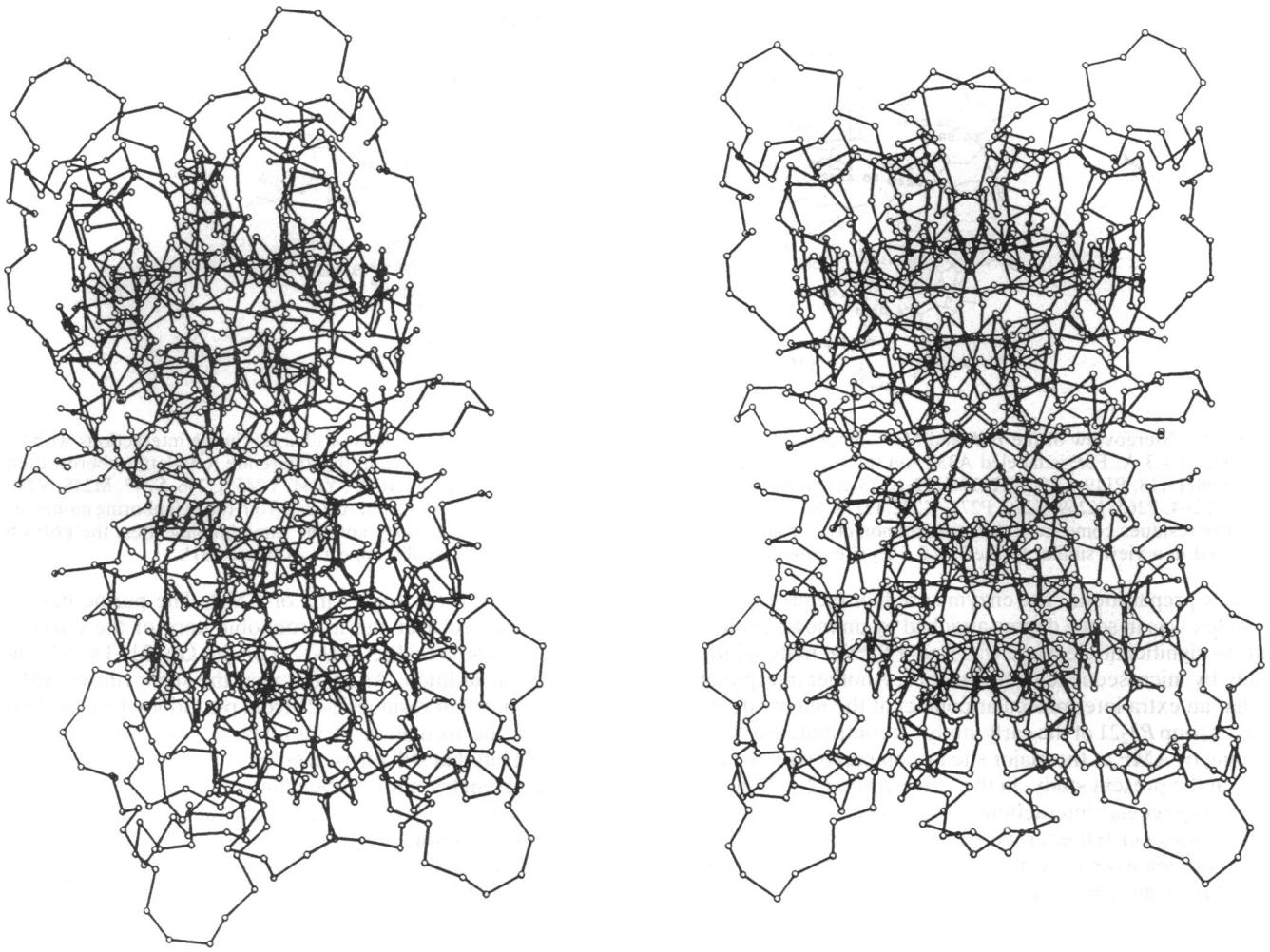

FIG. 3. Plots of Cα atoms of the tetramer viewing along the molecular twofold axis *p* (vertical in Fig. 1) for the enzyme–Fru-2,6-P_2 complex from the superposition onto the enzyme–F6*P*–AMP–Mg^{2+} complex (*Left*) and for the enzyme–F6*P*–AMP–Mg^{2+} complex (*Right*). Small circles represent the positions of Cα atoms. The C1 chain is located at the lower right of each drawing while the C2 chain is at the upper left. Dimers C1–C2 in the two structures were superimposed and hence have the same orientation. The C3 and C4 chains correspond to the lower left and upper right, respectively. The dimer C3–C4 is twisted about 19° about the molecular twofold axis *p* in the enzyme–F6*P*–AMP–Mg^{2+} structure, as compared with C3–C4 in the unligated enzyme or its complex with Fru-2,6-P_2.

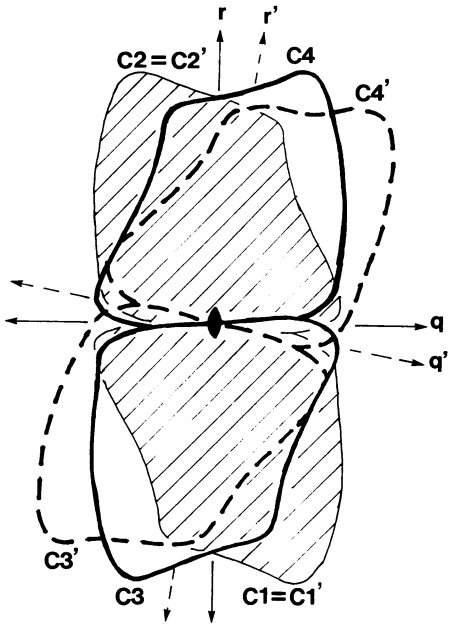

FIG. 4. Schematic drawing of the superposition of the enzyme–Fru-2,6-P_2 complex on the enzyme–F6*P*–AMP–Mg^{2+} complex viewed along the molecular twofold axis *p*. Dimers C1–C2 are superimposed and drawn as hatched regions. The heavy solid lines represent dimer C3–C4 of the enzyme–Fru-2,6-P_2 complex while the dashed lines are those of the enzyme–F6*P*–AMP–Mg^{2+} complex. Dimer C3–C4 of the F6*P*–AMP–Mg^{2+} complex is twisted about 19° about the molecular twofold axis *p* relative to the same dimer of the Fru-2,6-P_2 complex when the Fru-2,6-P_2 complex is transformed to the F6*P*–AMP–Mg^{2+} complex. Correspondingly, molecular twofold axes *q* and *r* rotate about 9.5° from the initial position (solid line) to the dashed line position.

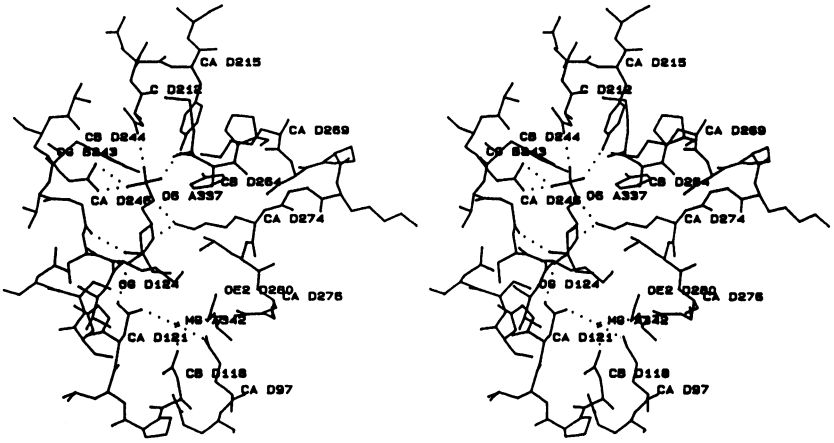

FIG. 5. Stereoview of the F6*P* and Mg^{2+} binding sites. Dotted lines represent the hydrogen bonds or charge–charge interactions within a distance of 3.3 Å. F6*P* is labeled A337 and the Mg^{2+} site is marked with an X. Amino acids shown in this figure are (one-letter abbreviation) E97, E98, D118, P119, L120, D121, G122, S123, S124, N125, N212, E213, G214, Y215, A216, A242, R243, Y244, V245, G246, S247, M248, V249, M263, Y264, P265, K269, S270, P271, K272, G273, K274, L275, R276, and E280. Except for Ala-242 and Arg-243 from the neighboring monomer, all other residues come from the same monomer. For an easy comparison that F6*P* and Fru-2,6-P_2 have the same binding sites, the F6*P* site is plotted in a view similar to the Fru-2,6-P_2 site (compare with figure 10 in ref. 8, which actually appears as figure 13)*.

enzyme preparations. The enzyme used for the previous AMP complex was in some degree attacked by unknown proteases, but no significant cleavage was found for the material in this study by microsequencing techniques. Another interpretation is that an extra intermolecular contact at the major site in the space group $P3_221$ of the early study (7) contributes to stronger binding of AMP at the major site as compared with the minor site. In the present study, in the space group $P2_12_12$, there are no intermolecular interactions with AMP.

Two sites per tetramer were reported for the AMP binding to the bovine liver enzyme (23, 24), but additional sites were observed if the concentration of AMP was raised to 0.2 mM (25). Four sites per tetramer were also observed (26–29). In the presence of substrate, occupation of these sites is enhanced (30, 31). Our results, four sites per tetramer for AMP binding to the neutral form of the pig kidney enzyme (this study) and two sites for AMP binding to the partially proteolytically cleaved form (7), are consistent with the kinetic observations that when the neutral form of the enzyme is subjected to proteolysis, the AMP inhibition is decreased or completely lost for the enzymes from rabbit liver (32–36), rat liver (36), chicken liver (37), sheep liver (38), and pig kidney (39).

As shown in Fig. 6, the phosphate group of AMP interacts with the backbone atoms of Glu-29 and Met-30 and side chain atoms of Thr-27, Lys-112, and Tyr-113 in both chains of the dimer. The side chain atoms of Tyr-113 in both chains are also in contact with the sugar ring of AMP. The purine base of AMP is located near the hydrophobic core of the enzyme, interacting with residues Val-17, Gln-20, Gly-21, Thr-31, and Met-177. In addition, Arg-140 is near the sugar ring of AMP.

The removal of residues 1–25 from pig kidney Fru-1,6-Pase results in the formation of an enzyme insensitive to AMP inhibition but that still turns over the substrate (40). Our AMP binding geometry shows abundant contacts between AMP and residues Val-17 to Thr-31 in accordance with the above kinetic observation.

The ultraviolet difference spectrum of Fru-1,6-Pase induced by AMP showed maxima at 288 and 279 nm, which were interpreted as perturbations in the environment of tyrosine residues (41). Our structures suggest that Tyr-113 may contribute to the spectral change. This tyrosine is conserved throughout all known sequences. In addition, residues Val-17, Met-30, Thr-31, and Met-177 show conservative variation. Arg-140 is conserved as either arginine or lysine in all AMP-binding Fru-1,6-Pases. Chemical modification of rabbit liver Fru-1,6-Pase with pyridoxal phosphate decreases its sensitivity to AMP inhibition; two lysyl residues were modified to the extent of ≈50% (42). Comparative sequence analyses have indicated that residue 141, which is lysine in the pig kidney enzyme and leucine in the yeast enzyme, is not a good candidate for the AMP binding (3, 6, 43); this result is in agreement with our structure studies.

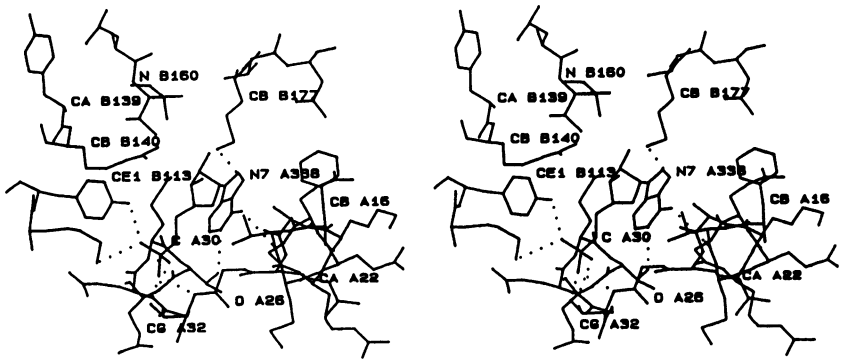

FIG. 6. Stereoplot of the AMP binding site. Dotted lines represent the hydrogen bonds or charge–charge interactions within a distance of 3.3 Å. AMP is labeled A338. Amino acids shown in this figure are (one-letter abbreviations) F16, V17, M18, E19, Q20, G21, R22, K23, A24, R25, G26, T27, G28, E29, M30, T31, Q32, K112, Y113, Y139, R140, L159, V160, A161, M177, V178, and N179. The α-helix feature of residues 16–24 is clearly seen in the low right corner. At the present level of resolution and refinement, the AMP fits the density in either the syn or anti conformation.

In contrast to the active site residues, the conservation of amino acids in the AMP binding site is poor, perhaps because residues 17–31 interact with AMP mainly through backbone atoms. Hence, a mutation of one or more side chains may have less effect on the AMP binding. On the other hand, sequence variation may reflect different levels of AMP inhibition in various species of the enzyme. For instance, the AMP inhibition of Fru-1,6-Pase can vary significantly, ranging from K_i values below 1 μM for the rabbit skeletal muscle enzyme (44), through 10–20 μM for the liver and kidney enzymes (45), 80–200 μM for the yeast enzymes (46), to no AMP inhibition for chloroplast (47, 48) and bumblebee flight muscle (49) enzymes.

Note Added in Proof. An additional sequence, from spinach chloroplast, has appeared (50) to supplement those sequences in refs. 1–6.

We thank Drs. S. Sobottka and R. Kretsinger for the use of the multiwire x-ray area detector at the Biotechnology Resource, University of Virginia, and Dr. F. Marcus of Chiron Corporation for the microsequencing of our crystals. We also thank the National Institutes of Health for Grant GM06920 and the Pittsburgh Supercomputing Center and National Science Foundation for support of the computing facilities.

1. Marcus, F., Edelstein, I., Reardon, I. & Heinrikson, R. L. (1982) *Proc. Natl. Acad. Sci. USA* **79,** 7161–7165.
2. Fisher, W. K. & Thompson, E. O. P. (1983) *Aust. J. Biol. Sci.* **36,** 235–250.
3. Rogers, D. T., Hiller, E., Mitsock, L. & Orr, E. (1988) *J. Biol. Chem.* **263,** 6051–6057.
4. Hamilton, W. D. O., Harrison, D. A. & Dyer, T. A. (1988) *Nucleic Acids Res.* **16,** 8707.
5. Raines, C. A., Lloyd, J. C., Longstaff, M., Bradley, D. & Dyer, T. (1988) *Nucleic Acids Res.* **16,** 7931–7942.
6. El-Maghrabi, M. R., Pilkis, J., Marker, A. J., Colosia, A. D., D'Angelo, G., Fraser, B. A. & Pilkis, S. J. (1988) *Proc. Natl. Acad. Sci. USA* **85,** 8430–8434.
7. Ke, H. M., Thorpe, C. M., Seaton, B. A., Marcus, F. & Lipscomb, W. N. (1989) *Proc. Natl. Acad. Sci. USA* **86,** 1475–1479.
8. Ke, H. M., Thorpe, C. M., Seaton, B. A., Lipscomb, W. N. & Marcus, F. (1990) *J. Mol. Biol.* **212,** 513–539.
9. Benkovic, S. J. & deMaine, M. M. (1982) *Adv. Enzymol.* **53,** 45–82.
10. Tejwani, G. A. (1983) *Adv. Enzymol.* **54,** 121–194.
11. Pilkis, S. J., Claus, T. H., Kountz, P. D. & El-Maghrabi, M. R. (1987) in *The Enzymes*, eds. Boyer, P. D. & Krebs, E. G. (Academic, New York), 3rd Ed., Vol. 18, pp. 3–46.
12. Van Schaftingen, E. (1987) *Adv. Enzymol.* **59,** 315–395.
13. Meek, D. W. & Nimmo, H. G. (1983) *FEBS Lett.* **160,** 105–109.
14. Taketa, K. & Pogell, B. M. (1965) *J. Biol. Chem.* **240,** 651–662.
15. Van Schaftingen, E. & Hers, H. G. (1981) *Proc. Natl. Acad. Sci. USA* **78,** 2861–2863.
16. Pilkis, S. J., El-Maghrabi, M. R., Pilkis, J. & Claus, T. H. (1981) *J. Biol. Chem.* **256,** 3619–3622.
17. Sobottka, S. E., Cornic, G. G., Kretsinger, R. H., Rains, R. G., Stephens, W. A. & Weissman, L. J. (1984) *Nucl. Instrum. Methods* **220,** 575–581.
18. Crowther, R. A. (1972) in *The Molecular Replacement Method*, ed. Rossmann, M. G. (Gordon and Breach, New York), pp. 173–178.
19. Machin, P. A. (1985) *Molecular Replacement,* Proceedings of the Daresbury Study Weekend (Daresbury Laboratory).
20. Jones, T. A. (1982) in *Computational Crystallography*, ed. Sayer, D. (Oxford, London), pp. 303–317.
21. Brünger, A. T., Kuriyan, J. & Karplus, M. (1987) *Science* **235,** 458–460.
22. Marcus, F., Harrsch, P. B., Moberly, L., Edelstein, I. & Latshaw, S. P. (1987) *Biochemistry* **26,** 7029–7035.
23. Nimmo, H. G. & Tipton, K. F. (1975) *Eur. J. Biochem.* **58,** 575–585.
24. Tejwani, G. A., Pedrosa, F. O., Pontremoli, S. & Horecker, B. L. (1976) *Arch. Biochem. Biophys.* **177,** 253–264.
25. Arneson, R. M., Geller, A. M. & Byrne, W. L. (1979) *Enzyme* **24,** 132–136.
26. Pontremoli, S., Grazi, E. & Accorsi, A. (1968) *Biochemistry* **7,** 3628–3633.
27. Kratowich, N. & Mendicino, J. (1974) *J. Biol. Chem.* **249,** 5485–5494.
28. Marcus, F. & Haley, B. E. (1979) *J. Biol. Chem.* **254,** 259–261.
29. McGrane, M. M., El-Maghrabi, M. R. & Pilkis, S. J. (1983) *J. Biol. Chem.* **258,** 10445–10454.
30. Sarngadharan, M. G., Watanabe, A. & Pogell, B. M. (1969) *Biochemistry* **8,** 1411–1419.
31. Benkovic, P. A., Frey, W. A. & Benkovic, S. J. (1978) *Arch. Biochem. Biophys.* **191,** 719–726.
32. Pontremoli, S., Melloni, E. & Traniello, S. (1971) *Arch. Biochem. Biophys.* **147,** 762–766.
33. Pontremoli, S., Melloni, E., De Flora, A. & Horecker, B. L. (1973) *Proc. Natl. Acad. Sci. USA* **70,** 661–664.
34. Traniello, S., Melloni, E., Pontremoli, S., Sia, C. L. & Horecker, B. L. (1972) *Arch. Biochem. Biophys.* **149,** 222–231.
35. El-Dorry, H. A., Chu, D. K., Dzugaj, A., Botelho, L. H., Pontremoli, S. & Horecker, B. L. (1977) *Arch. Biochem. Biophys.* **182,** 763–773.
36. Macgregor, J. S., Hannappel, E., Xu, G. J., Pontremoli, S. & Horecker, B. L. (1982) *Arch. Biochem. Biophys.* **217,** 652–664.
37. Cruz, Z. M., Tanizaki, M. M., El-Dorry, H. A. & Bacila, M. (1979) *Arch. Biochem. Biophys.* **198,** 424–433.
38. Zalitis, J. (1976) *Biochem. Biophys. Res. Commun.* **70,** 323–330.
39. Marcus, F., Edelstein, I., Saidel, L. J., Keim, P. S. & Heinrikson, R. L. (1981) *Arch. Biochem. Biophys.* **209,** 687–696.
40. Chatterjee, T., Reardon, I., Heinrikson, R. L. & Marcus, F. (1985) *J. Biol. Chem.* **260,** 13553–13559.
41. Pilkis, S. J., El-Maghrabi, M. R., McGrane, M. M., Pilkis, J. & Claus, T. H. (1981) *J. Biol. Chem.* **256,** 11489–11495.
42. Suda, H., Xu, G. J., Kutny, R. M., Natalini, P., Pontremoli, S. & Horecker, B. L. (1982) *Arch. Biochem. Biophys.* **217,** 10–14.
43. Marcus, F., Rittenhouse, J., Gontero, B. & Harrsch, P. B. (1987) *Arch. Biol. Med. Exp.* **20,** 371–378.
44. Black, W. J., Van Tol, A., Fernando, J. & Horecker, B. L. (1972) *Arch. Biochem. Biophys.* **151,** 576–590.
45. Colombo, G. & Marcus, F. (1973) *J. Biol. Chem.* **248,** 4923–4925.
46. Marcus, F., Rittenhouse, J., Moberly, L., Edelstein, I., Hiller, E. & Rogers, D. T. (1988) *J. Biol. Chem.* **263,** 6058–6062.
47. Preiss, J., Biggs, M. L. & Greenberg, E. (1967) *J. Biol. Chem.* **242,** 2292–2294.
48. Buchanan, B. B., Schurmann, P. & Kalberer, P. P. (1971) *J. Biol. Chem.* **246,** 5952–5959.
49. Newsholme, E. A., Crabtree, B., Higgins, S. J., Thornton, S. D. & Start, C. (1972) *Biochem. J.* **128,** 89–97.
50. Marcus, F. & Harrsch, P. B. (1990) *Arch. Biochem. Biophys.* **279,** 151–157.